



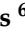

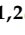


Article

# Calcium Signaling Alterations Caused by Epigenetic Mechanisms in Pancreatic Cancer: From Early Markers to Prognostic Impact

Cleandra Gregório <sup>1,2,†</sup> , Sheila Coelho Soares-Lima <sup>3,†</sup> , Bárbara Alemar <sup>1,†</sup>,  
Mariana Recamonde-Mendoza <sup>4,5</sup> , Diego Camuzi <sup>3</sup> , Paulo Thiago de Souza-Santos <sup>6</sup> ,  
Raquel Rivero <sup>7,8</sup>, Simone Machado <sup>7</sup>, Alessandro Osvaldt <sup>9,10,11</sup> , Patricia Ashton-Prolla <sup>1,2</sup>   
and Luis Felipe Ribeiro Pinto <sup>3,12,\*</sup>

<sup>1</sup> Laboratório de Medicina Genômica, Centro de Pesquisa Experimental, Hospital de Clínicas de Porto Alegre, Porto Alegre 90035-007, Brazil; cleandra.gregorio@gmail.com (C.G.); barbara.alemar@gmail.com (B.A.); pprolla@gmail.com (P.A.-P.)

<sup>2</sup> Programa de Pós-graduação em Genética e Biologia Molecular, Universidade Federal do Rio Grande do Sul, Porto Alegre 91501-970, Brazil

<sup>3</sup> Programa de Carcinogênese Molecular, Instituto Nacional de Câncer, Rio de Janeiro 20231-050, Brazil; sheilacoelho@gmail.com (S.C.S.-L.); drdcamuzi@gmail.com (D.C.)

<sup>4</sup> Instituto de Informática, Universidade Federal do Rio Grande do Sul, Porto Alegre 91501-970, Brazil; mrmendoza@inf.ufrgs.br

<sup>5</sup> Núcleo de Bioinformática, Hospital de Clínicas de Porto Alegre, Porto Alegre 90035-007, Brazil

<sup>6</sup> Laboratório de Hanseníase, Instituto Oswaldo Cruz, Fiocruz, Rio de Janeiro 21040-360, Brazil; pthiagoss@gmail.com

<sup>7</sup> Serviço de Patologia, Hospital de Clínicas de Porto Alegre, Porto Alegre 90035-007, Brazil; rrivero@hcpa.edu.br (R.R.); smsmachado@hcpa.edu.br (S.M.)

<sup>8</sup> Departamento de Patologia, Faculdade de Medicina, Universidade Federal do Rio Grande do Sul, Porto Alegre 90035-003, Brazil

<sup>9</sup> Grupo de Vias Biliares e Pâncreas, Cirurgia do Aparelho Digestivo, Hospital de Clínicas de Porto Alegre, Porto Alegre 90035-007, Brazil; aosvaldt@hcpa.edu.br

<sup>10</sup> Programa de Pós-graduação em Medicina: Ciências Cirúrgicas, Universidade Federal do Rio Grande do Sul, Porto Alegre 90035-007, Brazil

<sup>11</sup> Faculdade de Medicina, Universidade Federal do Rio Grande do Sul, Porto Alegre 90035-007, Brazil

<sup>12</sup> Departamento de Bioquímica, Instituto de Biologia Roberto Alcântara Gomes, Universidade do Estado do Rio de Janeiro, Rio de Janeiro 20550-900, Brazil

\* Correspondence: lfrpinto@inca.gov.br; Tel.: +55-21-3207-6598

† These authors contributed equally to this work.

Received: 29 April 2020; Accepted: 21 June 2020; Published: 30 June 2020



**Abstract:** Pancreatic ductal adenocarcinoma (PDAC) is an aggressive disease with high mortality rates. PDAC initiation and progression are promoted by genetic and epigenetic dysregulation. Here, we aimed to characterize the PDAC DNA methylome in search of novel altered pathways associated with tumor development. We examined the genome-wide DNA methylation profile of PDAC in an exploratory cohort including the comparative analyses of tumoral and non-tumoral pancreatic tissues (PT). Pathway enrichment analysis was used to choose differentially methylated (DM) CpGs with potential biological relevance. Additional samples were used in a validation cohort. DNA methylation impact on gene expression and its association with overall survival (OS) was investigated from PDAC TCGA (The Cancer Genome Atlas) data. Pathway analysis revealed DM genes in the calcium signaling pathway that is linked to the key pathways in pancreatic carcinogenesis. DNA methylation was frequently correlated with expression, and a subgroup of calcium signaling genes was associated with OS, reinforcing its probable phenotypic effect. Cluster analysis of PT samples revealed that some of the methylation alterations observed in the Calcium signaling pathway seemed to occur early in the carcinogenesis process, a finding that may open new insights about PDAC tumor biology.

**Keywords:** pancreatic ductal adenocarcinoma; calcium signaling pathway; DNA methylation; early methylation alterations; prognostic biomarkers

---

## 1. Introduction

Pancreatic cancer is a very aggressive disease, with 5-year survival rates below 8% and a strong ability to metastasize even before the primary tumor is clinically detected [1,2]. Tumor aggressiveness, lack of specific symptoms in early stages, and resistance to cytotoxic drugs, all contribute to the high mortality rates [3]. In fact, current estimates predict that pancreatic cancer will be the second most lethal tumor by 2030 [4]. Considering all pancreatic malignancies, pancreatic ductal adenocarcinoma (PDAC) is the most prevalent type, accounting for more than 90% of the cases [5]. PDAC initiation and progression are promoted by the interaction between driver mutations and the disruption of epigenetic regulatory circuits, such as DNA methylation [6].

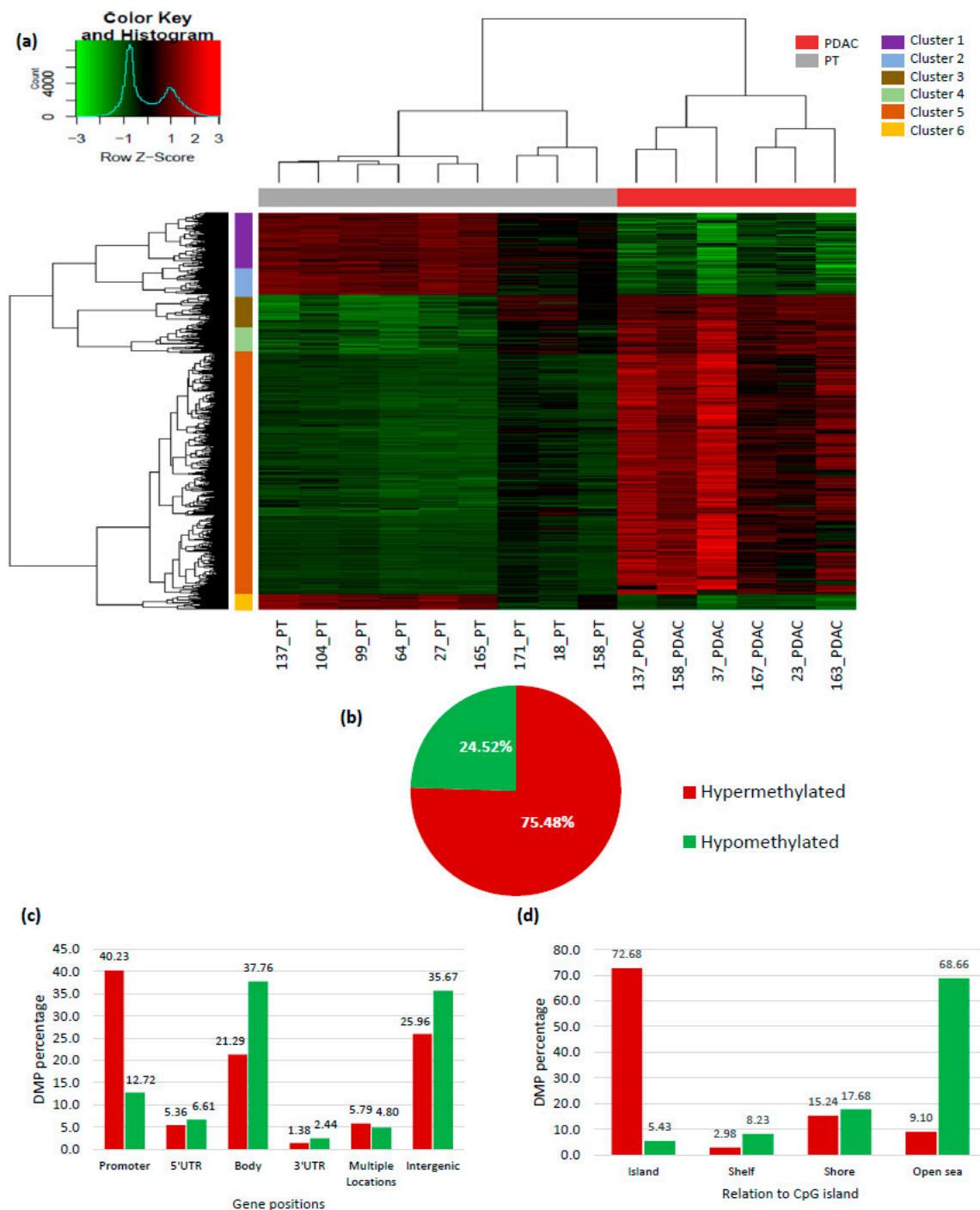
DNA methylation is one of the best understood epigenetic mechanisms of transcriptional regulation. In cancer, the DNA methylation landscape often involves global hypomethylation mainly described at CpG sites located in intergenic regions, including repetitive elements [7]. Alternatively, studies using RefSeq gene analysis (such as the 450 K BeadChip Array platform) show that most CpGs are hypermethylated in cancer, affecting mainly tumor suppressor genes [8,9]. However, there are only limited data on the wide DNA methylation patterns of PDAC [10,11].

The discovery of new biomarkers including DNA methylation and other biologic processes for the development of novel target-driven therapies, and the definition of prognosis in PDAC are urgent needs. In this study, we aimed to characterize the PDAC DNA methylome in search of novel altered pathways associated with tumor development through a comparative analysis of tumor and non-tumor pancreatic tissue (PT) samples. An important new finding resulting from this analysis was the identification of several differentially methylated genes of the calcium ( $\text{Ca}^{2+}$ ) signaling pathway, linked to key pathways in pancreatic carcinogenesis. In addition, some of the methylation alterations observed in this pathway seem to occur early in the carcinogenesis process, a finding that may open new insights about PDAC tumor biology.

## 2. Results

### 2.1. Genome-Wide DNA Methylation Profile in Pancreatic Adenocarcinoma

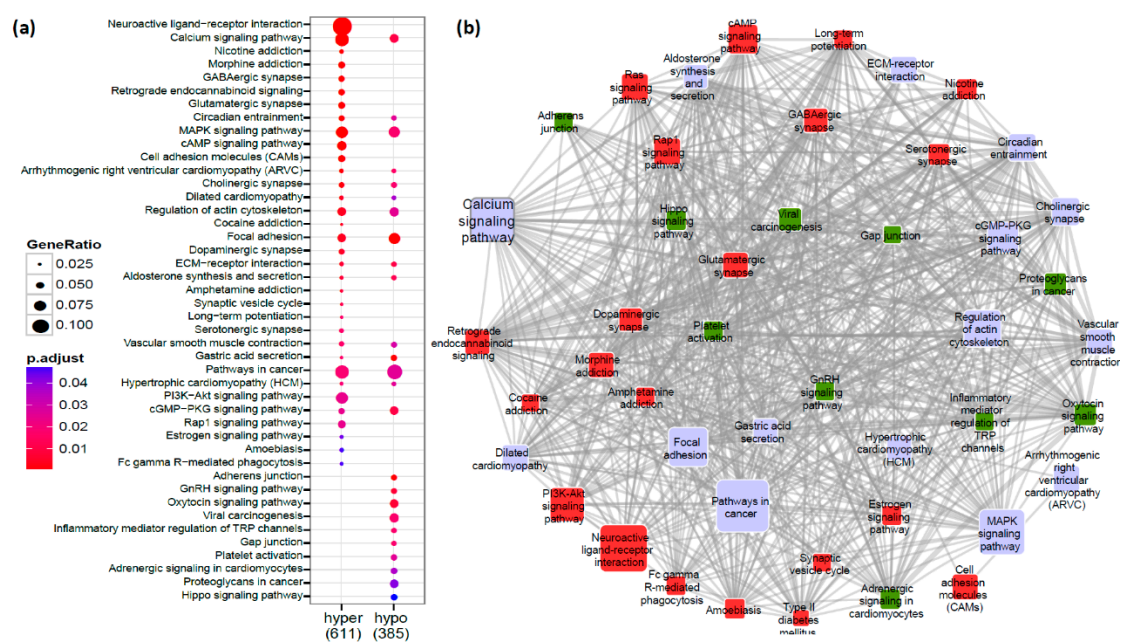
The genome-wide DNA methylation profile of six PDACs (with a minimum of 70% cellularity) compared to nine PT fresh frozen tissue samples was determined in an exploratory cohort using Infinium 450 K beadchips. The unsupervised hierarchical clustering analysis of the 10,361 differentially methylated probes (DMPs, adjusted  $p$ -value  $< 0.01$  and  $\Delta\beta \geq 0.2$ ) exhibited clear separation between the PDAC and PT. As shown in Figure 1a, two major clusters emerged: the first comprised PT samples and was predominantly hypomethylated, while the PDAC samples formed the second cluster that showed an overall hypermethylated profile (75.48% of the DMPs). PDAC hypermethylated probes were most frequently annotated to promoter regions (40.23%), while most hypomethylated probes were mapped to gene bodies (37.76%). Stratification by distance to CpG islands revealed that hypomethylated CpG sites most commonly encompassed open sea regions (68.66%), and hypermethylation was most common at CpG islands (72.68%) (Figure 1b–d).



**Figure 1.** DNA methylation profile of pancreatic ductal adenocarcinoma. (a) Heatmap showing the unsupervised hierarchical clustering of pancreatic ductal adenocarcinoma (PDAC, with a minimum 70% cellularity) and non-tumoral adjacent pancreatic tissue (PT) according to the methylation profile of the 10,361 probes found to be differentially methylated between groups (adjusted  $p$ -value < 0.01 and  $\Delta\beta \geq 0.2$ ). Hyper- and hypomethylation are represented in red and green, respectively. Colored bars on the left side of the heatmap represent probe clusters defined by their methylation similarities; (b) pie chart showing the percentage of hypomethylated and hypermethylated probes in PDAC relative to PT; (c) overall distribution of hypo- and hypermethylated probes according to their gene position; (d) overall distribution of hypo- and hypermethylated probes according to their relation to CpG islands.

## 2.2. $Ca^{2+}$ Pathway Genes Are Epigenetically Altered in PDAC

The next step was to analyze the potential biological relevance of the differentially methylated CpG sites identified in the supervised comparison between PDAC and PT samples. The DMPs mapped to 2715 genes, 1766 hypermethylated and 1100 hypomethylated, with an overlap of 151 genes among both sets. The set of 2715 genes had 611 hypermethylated and 386 hypomethylated genes annotated in the Kyoto Encyclopedia of Genes and Genomes (KEGG) database that were used as query gene sets to assess the functional enrichment of DMPs. Hypermethylated and hypomethylated genes were significantly associated with the enrichment of 36 and 25 cellular pathways, respectively (Figure S1a,b, Tables S1 and S2). Subsequently, we merged both analyses to identify the biological pathways that were frequently deregulated in PDAC by both hyper- and hypomethylation. As shown in Figure 2a, several pathways well known to be involved in cancer development were identified, such as the MAPK signaling pathway and the focal adhesion pathway [12,13]. Additionally, we observed that the  $Ca^{2+}$  signaling pathway had a large number of genes significantly hypo- and hypermethylated. This pathway is intrinsic to multiple aspects of cancer biology, such as tumor initiation, metastasis, and drug resistance [14]. The overlap between the differentially methylated genes of the  $Ca^{2+}$  signaling and other cellular pathways was investigated, and revealed that several of them were shared with other significantly enriched pathways, such as the Hippo and Ras signaling pathways (Figure 2b).

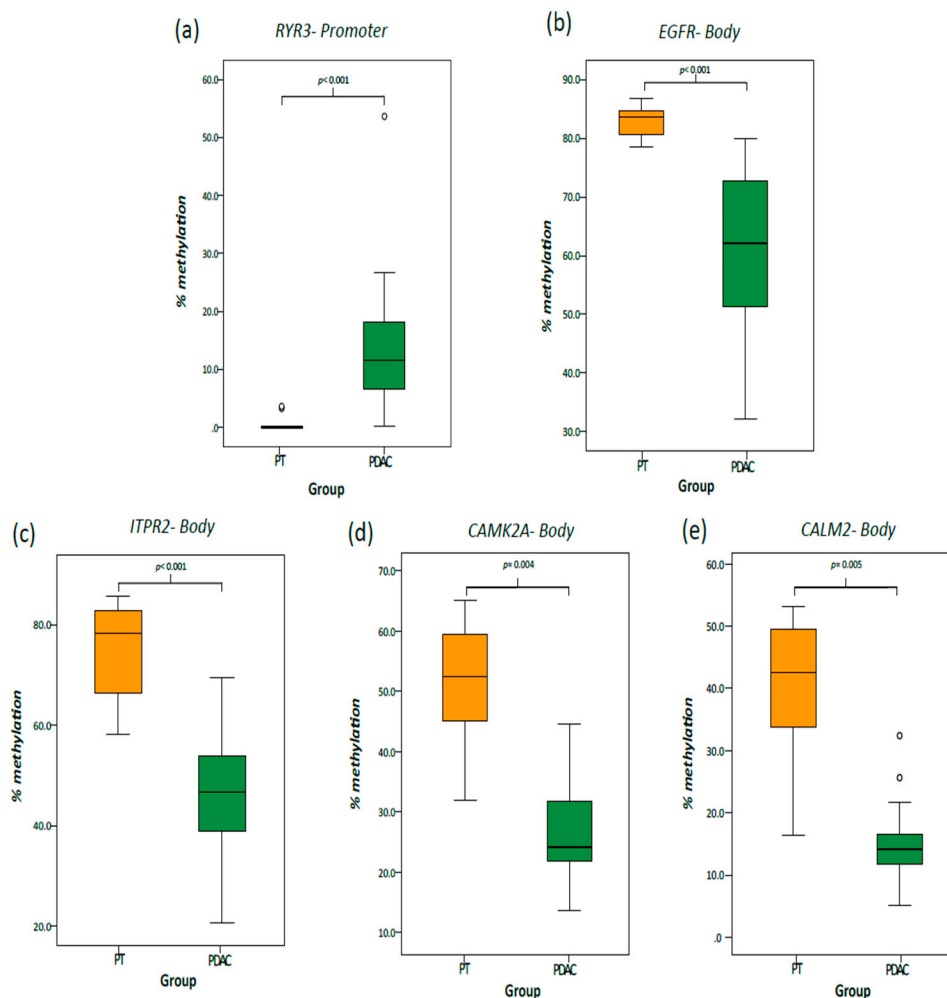


**Figure 2.** Pathway enrichment analysis of differentially methylated genes ( $n = 996$ ) in pancreatic ductal adenocarcinoma. (a) Functional enrichment of the hypermethylated ( $n = 611$ ) and hypomethylated genes ( $n = 385$ ) annotated from the differentially methylated probes (DMPs); (b) interactions between the enriched pathways evidencing the number of shared differentially methylated genes. The pathways in red and green are those enriched for hyper- and hypomethylated genes, respectively, and those in lilac are enriched for both methylation profiles.

## 2.3. Validation Cohort

The methylation profile of five genes were assessed in a validation cohort made of 43 PDAC and 24 PT samples, with the clinical features of patients shown in Table S3. The five genes were selected with the following criteria: those with a previously described role in cancer and containing DMPs associated with a high  $|\Delta\beta|$ . One hypermethylated promoter (*RYR3*, Ryanodine Receptor 3) and four hypomethylated gene body probes (*EGFR*, Epidermal Growth Factor Receptor; *ITPR2*, Inositol 1,4,5-Trisphosphate Receptor Type 2; *CAMK2A*, Calcium/Calmodulin Dependent Protein Kinase II

Alpha; and *CALM2*, Calmodulin 2) were chosen. Methylation levels at the CpG sites interrogated by the Infinium probe as well as surrounding CpG sites were evaluated, and the  $\beta$ -values obtained by pyrosequencing were strongly correlated with the Infinium assay (Figures 3 and S2).



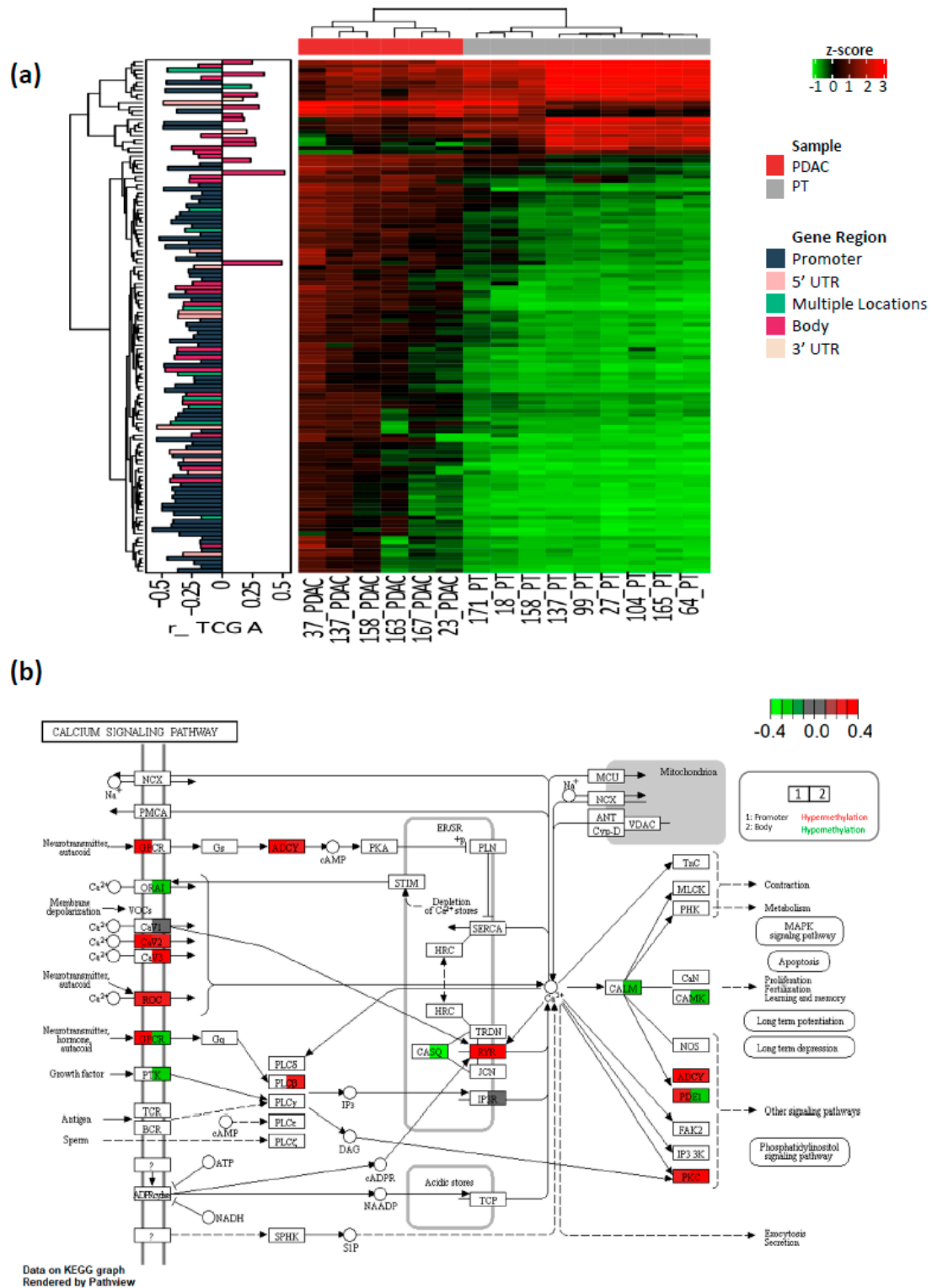
**Figure 3.** Validation of the genome-wide DNA methylation results by pyrosequencing. Boxplots represent the overall methylation of pancreatic adenocarcinoma (PDAC,  $n = 43$ ) and non-tumoral adjacent pancreatic tissue (PT,  $n = 24$ ) samples for the following genes: (a) *RYR3* (promoter); (b) *EGFR* (gene body); (c) *ITPR2* (gene body), (d) *CAMK2A* (gene body); and (e) *CALM2* (gene body).

#### 2.4. Correlation between Methylation and Expression of $Ca^{2+}$ Pathway Genes

The methylation profile of five genes were assessed in a validation cohort made of 43 PDAC and 24 PT samples, with the clinical features of patients shown in Table S3. The information available in TCGA (The Cancer Genome Atlas) about PDAC was used to explore the impact of DNA methylation on the expression of the  $Ca^{2+}$  signaling pathway genes [15]. Among 173 DMPs in the  $Ca^{2+}$  pathway genes, 112 (64.73%) showed a significant correlation with gene expression (Table S4). The bars located on the left side of the heatmap (Figure 4a) indicate the correlation coefficient per gene region affected. The methylation levels of probes annotated to promoters were significantly and inversely correlated with the expression in 62.3% of the comparisons. Comparatively, the methylation profile of probes located in gene bodies showed a correlation with an expression of 59.6% in the comparisons, 64.3% inverse and 35.7% positive.

In Figure 4b, a schematic diagram of the  $Ca^{2+}$  signaling pathway based on the KEGG database shows groups of genes (grouped within boxes by function, as indicated in Table S4) with significant correlations between methylation and expression. Colored boxes indicate the differential methylation

in the promoters and gene bodies identified in the present study. Genes that control intracellular  $Ca^{2+}$  storage, such as ryanodine receptors (*RYR2*, Ryanodine Receptor 2, and *RYR3*), were hypermethylated (promoters and gene bodies), while the inositol 1,4,5- trisphosphate receptor (*ITPR1*, Inositol 1,4,5-Trisphosphate Receptor Type 1) showed a heterogeneous DNA methylation profile in the body region.



**Figure 4.** Calcium ( $Ca^{2+}$ ) signaling pathway analysis. (a) Heatmap showing the methylation profile of the probes ( $n = 112$  probes) annotated to genes involved in the  $Ca^{2+}$  signaling pathway for which a

significant correlation (false discovery rate (FDR)-adjusted  $p$ -value  $< 0.05$ ) with a gene expression was observed in the TCGA dataset (The Cancer Genome Atlas,  $n = 141$ ). Heatmap was built based on the methylation data generated in the present study. The bars located on the left side of the heatmap indicate the correlation coefficient per gene region affected by differential methylation, and is based on the TCGA data; (b) schematic diagram of the  $\text{Ca}^{2+}$  signaling pathway. The network was built based on the Kyoto Encyclopedia of Genes and Genomes (KEGG) pathway map (KEGG: hsa04020). Each box represents a group of gene products (mostly protein) that have a common function, and its nomenclature can include one or many gene products. Gene products regarding each box are represented in Table S4.  $\text{Ca}^{2+}$  signaling pathway genes for which a significant correlation between methylation and expression was observed are highlighted showing the differential methylation in promoters and gene bodies identified in the present study. The red squares indicate hypermethylated genes while the green squares represent hypomethylated genes. UTR: Untranslated Region.

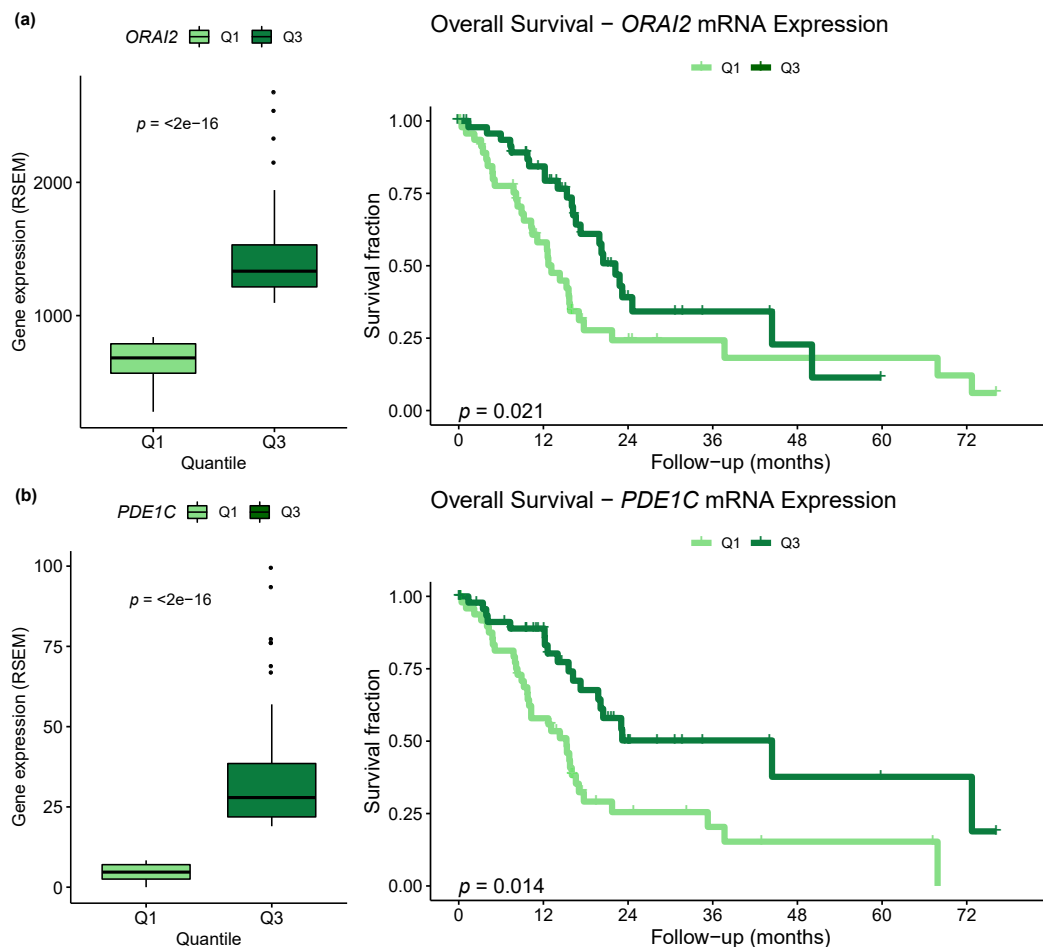
### 2.5. Differential Expression of $\text{Ca}^{2+}$ Pathway Genes Is Potentially Associated with Survival

$\text{Ca}^{2+}$  pathway genes that displayed significant correlations between methylation and expression in TCGA pancreatic cancer samples (Table S4) were selected for survival analysis. We evaluated the expression impact of 40 genes on a PDAC patient's overall survival (OS) (Table S5), including two genes that had already been investigated in the validation cohort (*CALM2*, and *RYR3*).

In the TCGA dataset ( $n = 146$ ), pathologic N stage (N1 vs. N0, Hazard Ratio (HR) = 1.832 (1.039–3.23 95%CI),  $p = 0.0364$ ) and residual tumor status after surgical resection (R1 vs. R0, HR = 1.899 (1.152–3.131 95%CI),  $p = 0.012$ ) were associated with OS, and remained in the model.

In the univariate analysis, PDAC patients with high *ADRA1A* (Adrenoceptor Alpha 1A), *CACNA1A* (Calcium Voltage-Gated Channel Subunit Alpha1 A), *CACNA1B* (Calcium Voltage-Gated Channel Subunit Alpha1 B), *CACNA1H* (Calcium Voltage-Gated Channel Subunit Alpha1 H), *CASQ2* (Calsequestrin 2) *ORAI2* (ORAI Calcium Release-Activated Calcium Modulator 2), *P2RX2* (Purinergic Receptor P2X 2), *PDE1C* (Phosphodiesterase 1C), and *PRKCB* (Protein Kinase C Beta) expression showed increased OS when compared to those with a low expression (Table S5). Conversely, decreased *HRH1* (Histamine Receptor H1) expression was associated with increased OS (Table S5).

After COX regression, the *ORAI2* (adjusted HR = 0.5004 (0.278–0.9009 95%CI), adjusted  $p = 0.021$ ) and *PDE1C* (adjusted HR = 0.4625 (0.2493–0.8577 95%CI), adjusted  $p = 0.0144$ ) higher expressions were shown to be independent variables associated with a better OS (Figure 5, Table S5).



**Figure 5.** Impact of the expression of  $\text{Ca}^{2+}$  signaling genes on PDAC overall survival. mRNA expression of selected genes was divided by tertiles, and the lower (Q1) and higher (Q3) tertiles were used to classify the cases into low and high expression, respectively. The adjustments were performed for pathologic N stage and residual tumor status after surgical resection. (a) On the left side of the Figure, the boxplot representing the expression profile of *ORAI2* in the low (Q1) and high (Q3) expression groups of PDAC patients. On the right side, the Kaplan–Meier survival curve shows the differences between the groups. Hazard Ratio (HR) = 0.5004 (0.278–0.9009 95%CI),  $p = 0.021$ . (b) On the left side of the Figure, the boxplot representing the expression profile of *PDE1C* in the low (Q1) and high (Q3) expression groups of PDAC patients. On the right side, the Kaplan–Meier survival curve shows the differences between the groups. HR = 0.4625 (0.2493–0.8577 95%CI),  $p = 0.0144$ . RSEM, RNA-Seq by Expectation-Maximization.

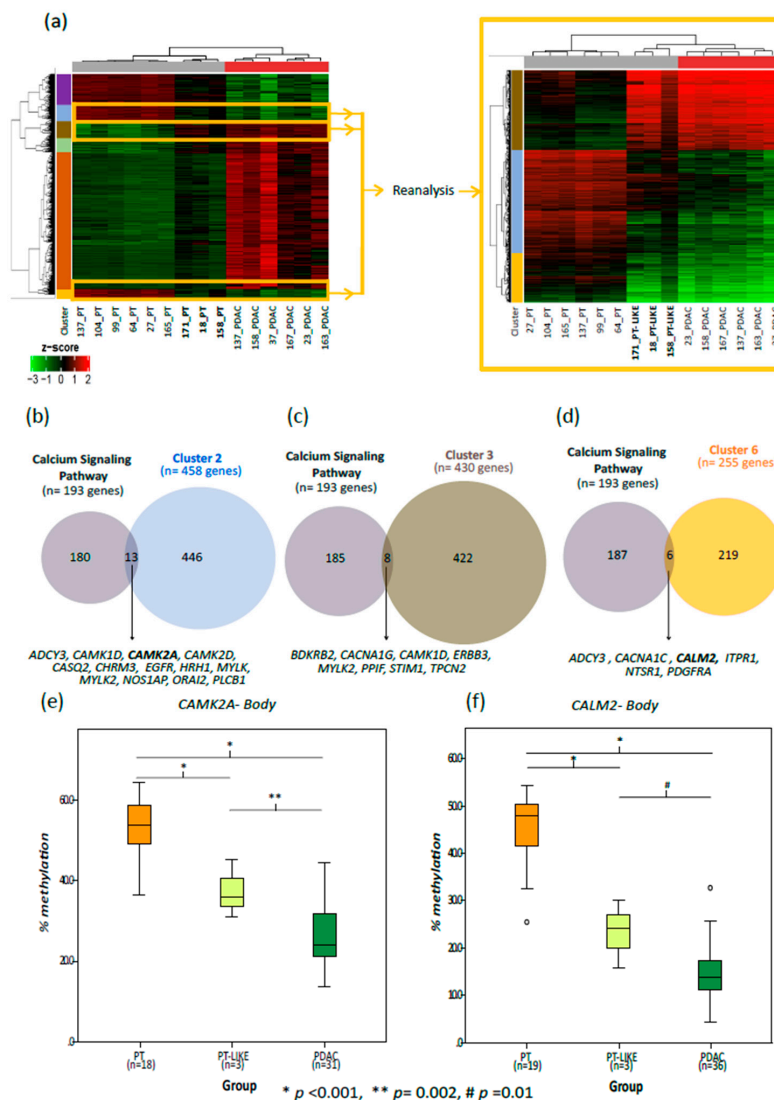
## 2.6. Aberrant Methylation in $\text{Ca}^{2+}$ Genes Is an Early Change in Pancreatic Cancer

We investigated the overall methylation profile of three PT samples (18 PT, 158 PT, and 171 PT) with intermediate methylation levels at the DMPs between PDAC and PT (Figure 1a, these samples will be named PT-like from now on). To validate this discordant methylation profile, first a multidimensional scaling plot was used, showing that PT-like samples were more closely related to PDAC than PT samples, when considering principal component 1 (Figure S3a). This finding may be associated with molecular field cancerization, since these samples showed a high percentage of normal ducts (>80%), small focal fibrosis regions, and no evidence of neoplastic cell contamination (Figure S3b–d).

Field cancerization is defined by a set of genetic and epigenetic alterations that indicate that a specific tissue area is undergoing a transformation process, or has a predisposition to initiate such a process, and this may occur without overt morphological changes [16]. Considering that this process occurred in PT-like samples, we performed a deep analysis of DMP clusters, comparing the major



similarities between PDAC and PT-like. Three clusters derived from the previous unsupervised hierarchical clustering analysis were selected for further investigation, namely, clusters 2, 3, and 6. After a new unsupervised hierarchical clustering analysis, using only the DMPs of these clusters, the PT-like samples were grouped with PDAC samples (Figure 6a). Then, we performed the pathway enrichment analysis with the corresponding annotated genes and observed that 24 differentially methylated genes were involved in the Ca<sup>2+</sup> signaling pathway: thirteen genes from cluster 2, eight from cluster 3, and six from cluster 6; and three genes appeared in more than one cluster (Figure 6b–d, Table S6). The stepwise methylation profile in the PT, PT-like and the PDAC samples was observed in two previously validated genes (*CALM2* and *CAMK2A*, Figure 6e,f) as well as in other 22 genes from the Ca<sup>2+</sup> signaling pathway (Figure S4).



**Figure 6.** Comparative DNA methylation analysis of the PT, PT-like and the PDAC samples. **(a–d)** Tissue samples with  $\geq 70\%$  cellularity. **(a)** Heatmaps highlighting the methylation profile of the probe clusters supposed to be altered in early stages of PDAC development. Heatmap on the left shows the 10,361 DMPs between the PDAC and PT. Clusters 2, 3 and 6 were selected for a detailed analysis (heatmap on the right) since their probes showed intermediate methylation levels (between PDAC and PT) in the PT-like samples; **(b–d)** the overlap between the genes involved in the calcium signaling pathway and the genes belonging to each selected probe cluster ((b) cluster 2; (c) cluster 3; and (d) cluster 6). **(e,f)** The boxplots representing the overall methylation level of *CALM2* (e) and *CAMK2A* (f) in the PT, PT-like and the PDAC samples ( $\geq 20\%$  cellularity). *p*-values were calculated using the generalized estimating equations.

### 3. Discussion

In this study, we used a genome-wide DNA methylation approach to identify new pathways associated with PDAC development. Pathway enrichment analysis revealed the differentially methylated genes of the  $\text{Ca}^{2+}$  signaling pathway. Moreover, we showed aberrant DNA methylation patterns in a few PT samples indicating the possible formation of field cancerization. Nones et al. and Mishra et al. previously used the 450 K BeadChip Array to build two PDAC methylome databases, and similar to our data (Figure 1b), they showed that the majority of DMPs in PDAC were hypermethylated (56.59% and 50.59%, respectively) and located in promoter regions [10,11]. CpG island methylation in promoters is frequently associated with gene silencing during tumorigenesis, providing an alternative mechanism to mutations by which tumor suppressor genes may be inactivated within a cancer cell [17,18]. In our exploratory cohort, as well as in other studies, the Tumor Suppressor Genes (TSGs) *NPTX2* (Neuronal Pentraxin 2), *CDO1* (Cysteine Dioxygenase Type 1), *TFPI2* (Tissue Factor Pathway Inhibitor 2), *SFRP1* (Secreted Frizzled Related Protein 1), *SFRP2* (Secreted Frizzled Related Protein 2), *PENK* (Proenkephalin) and *FOXE1* (Forkhead box E1) had a remarkable hypermethylation pattern in the PDAC group [19–24].

Key signaling pathways involved in cancer were identified as differentially methylated in our study, e.g., the MAPK signaling pathway, which is engaged in multiple proliferative cellular processes (cell differentiation, proliferation, and apoptosis) [12], and the focal adhesion pathway, which may play a role in the development and progression of cancer [13]. In addition, we observed that the  $\text{Ca}^{2+}$  signaling pathway had a high number of genes both significantly hypo- and hypermethylated (Figure 2a).  $\text{Ca}^{2+}$  is a ubiquitous intracellular messenger that controls diverse processes in cellular physiology, such as gene transcription, cell progression, cell motility, and apoptosis [25]. Although  $\text{Ca}^{2+}$  pathway methylation in PDAC is still poorly explored, many of its genes have already been described as differentially methylated in other solid tumors, including gastric [8], prostate [8,26], and breast cancer [8,26]. Resting cytosolic free  $\text{Ca}^{2+}$  is maintained at lower levels than those of extracellular space, and its equilibrium dynamics is carefully regulated by the plasmatic membrane, endoplasmic reticulum (ER), and mitochondria [27], using a “toolkit” of channels, pumps, and cytosolic buffers to control  $\text{Ca}^{2+}$  cell homeostasis [28]. The spatial and temporal dynamics of  $\text{Ca}^{2+}$  signaling results in specific cellular responses mediated by the activation of a subset of  $\text{Ca}^{2+}$ -dependent effectors [29].

During carcinogenesis, several cellular metabolic functions become deregulated, including those related to  $\text{Ca}^{2+}$  signaling [30,31], and therefore, it is not surprising that changes in the expression or function of  $\text{Ca}^{2+}$  handling proteins impact tumorigenesis. In fact, different tumors present altered expression or mutations in the genes involved in  $\text{Ca}^{2+}$  signaling [32–36]. Different  $\text{Ca}^{2+}$  channels or pumps are potential therapeutic targets in different cancer subtypes, and are correlated with prognosis [8,32,37,38]. In our study, we showed that altered methylation levels of *ADRA1A*, *CACNA1A*, *CACNA1B*, *CACNA1H*, *CASQ2*, *HRH1*, *ORAI2*, *P2RX2*, *PDE1C*, and *PRKCB*, had an impact on their expression (Table S4). Furthermore, *PDE1C* promoter hypermethylation (Table S4, positive  $\Delta\text{beta}$ , and negative  $r$  correlation) and *ORAI2* gene body hypomethylation (Table S4, negative  $\Delta\text{beta}$ , and negative  $r$  correlation) resulted in their downregulated expression in PDAC samples, identified as independent predictors of lower overall survival (Figure 5 and Table S5). Although we did not perform protein expression analyses (due to the limitation of the tissue samples available), the correlation between DNA methylation and mRNA expression, and the consequent impact on prognosis, which suggests a phenotypic importance of this finding. Interestingly, *ORAI2* controls  $\text{Ca}^{2+}$  influx through the plasmatic membrane [32,39,40].

Scarce information is available regarding the methylation-related expression deregulation of genes involved in the  $\text{Ca}^{2+}$  signaling pathway in PDAC. In one of the few studies, the methylation profile of *S100A4* (S100 Calcium Binding Protein A4), a  $\text{Ca}^{2+}$ -binding protein previously implicated in metastasis [41], was evaluated in PDAC samples and cell lines. Hypomethylation was detected in tumors, whereas all normal pancreatic tissue samples analyzed were hypermethylated in the same region. Moreover, gene and protein expression patterns were correlated with the methylation profile,

and were associated with poor tumor differentiation [42]. In addition, methylation patterns of *PCDH10* (Protocadherin 10), a member of the non-clustered protocadherin family that plays an important role in  $\text{Ca}^{2+}$ -dependent cell–cell signal transduction and adhesion, was investigated in PDAC cell lines (Capan-1, Panc-1, AsPC-1 and BxPC-3). *PCDH10* promoter methylation was observed in 50% of the cell lines studied and resulted in a marked reduction of its expression [43]. Later, this tumor suppressor gene was investigated in other PDAC cell lines and, as expected, the *PCDH10* promoter methylation again correlated with reduced protein expression. This study also showed high methylation levels in clinical samples ( $n = 23$ ), and the presence of this methylation pattern was associated with reduced progression-free survival [44]. Using the TCGA data, Mishra et al. analyzed a genome-wide DNA methylation profile, and although the genes of the  $\text{Ca}^{2+}$  signaling pathway occupied the fourth position in the functional enrichment of differentially methylated probes, this finding was not further explored [11]. In addition, also using the TCGA data, another study combined the methylation and expression data of twelve solid tumors (no PDAC included) in order to identify common patterns of methylation. Alterations in the  $\text{Ca}^{2+}$  signaling pathway were observed in nine cancer types and *AGTR1*, *GRIN2A* (Glutamate Ionotropic Receptor NMDA Type Subunit 2A), *ITPKB* (Inositol-Trisphosphate 3-Kinase B), and *SLC8A3* (Solute Carrier Family 8 Member A3) were repressed by hypermethylation in six of them [8].

Cytoplasmic  $\text{Ca}^{2+}$  concentrations rise in response to a variety of stimuli that activate  $\text{Ca}^{2+}$  channels in the plasma membrane (as ORAI, CaV1,2 and 3), or by release from intracellular stores through stromal interaction molecule (STIM), inositol 1,4,5-trisphosphate receptors ( $\text{IP}_3\text{R}$ ), and ryanodine receptors (RYRs). *ORAI2*, *CACNA1C* (Calcium Voltage-Gated Channel Subunit Alpha1 C), *CACNA1G* (Calcium Voltage-Gated Channel Subunit Alpha1 D), *STIM1* (Stromal interaction molecule 1) and *ITPR1* (Inositol 1,4,5-Trisphosphate Receptor Type 1) had an altered methylation profile in the PT-like samples (Figures 6b–d and S4). ORAI1 and STIM1 are known as calcium release-activated calcium (CRAC) channels [45]. In PDAC cell lines, they are overexpressed and play a pro-survival anti-apoptotic role in this tumor [46]. In a recent study, Khan et al. have demonstrated that PDAC proliferation suppression is possible by targeting the CRAC channel with RP4010, a CRAC channel inhibitor [47]. Growth factors binding to tyrosine kinase receptors (e.g., epidermal growth factor receptor, EGFR) and G protein-coupled receptors (GPCRs; e.g., histamine receptor H1, HRH1) control the intracellular  $\text{Ca}^{2+}$  by plasma membrane. After binding, phospholipase C is activated and promotes the generation of inositol-1,4,5-trisphosphate ( $\text{IP}_3$ ) and diacylglycerol, which lead to the release of  $\text{Ca}^{2+}$  from the ER into the cytosol by intracellular channels (such as ITPR1 and ITPR2) [48]. In addition to ITPR2, EGFR is frequently mutated or overexpressed in various cancer types [49,50], and in PDAC particularly, EGFR is essential for KRAS-driven pancreatic carcinogenesis [51–53]. It is known that KRAS-activating mutations are early events in PDAC carcinogenesis and occur in ~90% of cases [54]. RAS proteins can also activate phospholipase C and generate  $\text{IP}_3$ , leading to  $\text{Ca}^{2+}$  influx, so the most frequently mutated gene in PDAC is directly linked to  $\text{Ca}^{2+}$  signaling.

RYRs represent another way to control  $\text{Ca}^{2+}$  ER store, and in this study, *RYR2* and *RYR3* were found hypermethylated in PDAC, and their methylation levels were inversely correlated with mRNA expression (Table S4). These receptors are regulated by  $\text{Ca}^{2+}$  voltage channels and by various ions, molecules and proteins, e.g.,  $\text{Ca}^{2+}$ ,  $\text{Mg}^{2+}$ , calmodulin (CALM),  $\text{Ca}^{2+}$ /calmodulin-dependent protein kinase II (CAMK2), and nicotine [55,56]. Once  $\text{Ca}^{2+}$  levels rise in the cytoplasm, they are strictly controlled by CALM.  $\text{Ca}^{2+}$  binding dramatically changes the conformation of CALM and increases its affinity for a large number of CALM-binding proteins, including the multifunctional CALM kinases such as CAMK2 [57]. CAMK2 phosphorylates nearly 40 different proteins, including enzymes, ion channels, kinases, and transcription factors [58], and it is overexpressed in digestive cancers, such as colorectal cancer [59,60]. Epithelial–mesenchymal transition (EMT), one of the cancer hallmarks, is also controlled by  $\text{Ca}^{2+}$  levels through CAMK2A. Focal adhesion kinase (FAK), which increases the turnover of cell–cell contacts, is phosphorylated by CAMK2 and is consequently upregulated [61]. It is important to mention that the FAK pathway was differentially methylated in our analysis (Figure 2a).

On top of its association with different aspects of cancer cell biology and its crosstalk with other key signaling pathways, a role for the activation of  $\text{Ca}^{2+}$  signaling in therapy resistance has also been proposed. The mechanisms involved include the induction of multi-drug resistance (MDR) proteins via the  $\text{Ca}^{2+}$ -dependent transcription factor NFAT and the acquisition of stemness phenotypes by the induction of pluripotency genes and EMT [62–64]. In pancreatic cancer, ORAI3 and STIM1 (key components of store operated calcium entry—SOCE) have been shown to be required for TGF- $\beta$ -dependent SNAIL transcription [65] and TGF- $\beta$  signaling has already been associated with stroma-mediated drug resistance [66]. The EMT induction of pancreatic cells can also be mediated by acid-sensing ion channels (ASICs). ASICs sense the extracellular acidification (common in pancreatic cancer) and in response, increase intracellular  $\text{Ca}^{2+}$  levels and activate RhoA signaling [64]. Furthermore, Na(+)/H(+) exchangers, such as NHE1 (sodium/proton exchanger 1), interact with calmodulin in a  $\text{Ca}^{2+}$ -dependent manner and become activated, promoting intracellular alkalization and extracellular acidification [67]. Therefore, a complex positive feedback loop involving  $\text{Ca}^{2+}$  signaling, TGF- $\beta$ , and microenvironment acidification might be involved in EMT induction and, consequently, therapy resistance in pancreatic cancer.

It is important to mention that extracellular acidification is also involved in immune escape, which has been associated with lymph node metastasis in pancreatic cancer and is being explored as one of the most promising targets for therapy in cancer [64,68,69]. Besides the previously mentioned mechanisms of microenvironment acidification, KRAS mutations and the consequent activation of MAPK and PI3K-mTOR signaling can lead to GLUT1 upregulation. This glucose transporter can also be induced by nutrient deprivation and hypoxia. Consequently, high rates of aerobic glycolysis result in lactate production and microenvironment acidification. This not only blocks lactate export by T-cells, which also use aerobic glycolysis as an energetic source, but also downregulates interferon  $\gamma$  (IFN- $\gamma$ ) production by T-cells and natural killer cells, and polarizes macrophages to an immunosuppressive phenotype [70]. At the same time, tumor cells can cope with high extracellular acidification by modulating the expression of pH-regulating proteins and they can also use lactate as an alternative energetic source [70]. Hypoxia and the glycolytic metabolism were also associated with a wide range of epigenetic alterations both in tumor and immune cells within the tumor microenvironment, as shown in different cancer models, and HIF-2 $\alpha$  (hypoxia-inducible factor 2 alpha) interaction with beta-catenin was recently shown in pancreatic cancer [71,72]. Indeed, immune tolerance and lymph node invasion have also been linked to the activation of the Wnt signaling pathway in PDAC [68,73]. This pathway is one of the central players in the acquisition of stemness phenotypes and one of its non-canonical forms involves  $\text{Ca}^{2+}$  signaling [74]. Altogether, these data suggest another connection between the alterations identified in the present study, immune escape and local dissemination in PDAC.

Based on the widespread dysregulation of  $\text{Ca}^{2+}$  signaling in tumors and on its impact on different steps of tumor development and progression,  $\text{Ca}^{2+}$  signaling receptors have been suggested as therapeutic targets for different types of cancer. The blockage of TRPVs (transient receptor potential vanilloid channels), T-type  $\text{Ca}^{2+}$  channels, ORAIs and TRPCs (transient receptor potential channels) have been shown to suppress the proliferation/invasion and induce cell death in different cancer models [75]. In this context, the drug repurposing of already available blockers of SOCE and T-type  $\text{Ca}^{2+}$  channels have been evaluated [76,77]. Conversely, the activation of overexpressed targets may also be an alternative for inducing cell death, as shown in breast and prostate cancer [78,79]. Therapy targeting the  $\text{Ca}^{2+}$  signaling pathway in combination with conventional chemo or radiotherapy has also been proposed. Chemotherapy drugs approved for pancreatic cancer treatment, such as Fluorouracil (5-FU) and platins, have been tested in combination with ORAI1 (ORAI Calcium Release-Activated Calcium Modulator 1) silencing and T-type  $\text{Ca}^{2+}$  channels blockers in hepatocellular carcinoma and ovarian cancer, respectively, with promising effects [80,81]. Nevertheless, our findings suggest that in vitro studies should be carried out to understand the role of  $\text{Ca}^{2+}$  pathway altered genes in pancreatic carcinogenesis before pre-clinical assays with some of these drugs are developed.

Another relevant aspect to be considered before proposing a targeted therapy against the  $\text{Ca}^{2+}$  signaling pathway is its participation in the maintenance of different physiological systems. Therefore, although  $\text{Ca}^{2+}$  signaling represents a complex pathway involved in the establishment of different cancer phenotypes, and its therapeutic targeting seems promising, it might result in a plethora of side effects. In this context, and based on the widespread alterations of DNA methylation affecting different central signaling pathways in pancreatic cancer as shown here, epigenetic therapy may represent an alternative option. This is especially relevant because a crosstalk between  $\text{Ca}^{2+}$  signaling and DNA methylation has already been described.  $\text{Ca}^{2+}$  signaling is essential to initiating epigenetic reprogramming in early embryogenesis [82], and candidate epigenetic drugs have been shown to induce the reactivation of TSGs and cell death via a  $\text{Ca}^{2+}$ /CAMK-dependent pathway [38]. In addition to TSGs reactivation, DNA methylation inhibitors have also been shown to induce the expression of cancer-testis genes and transposable elements in cancer cells, resulting in the expression of neoantigens and in a viral mimicry state [83–85]. These effects, together with the reprogramming of exhausted T-cells, put epigenetic therapy as a very promising approach in combination with immune checkpoint blockade for PDAC [85].

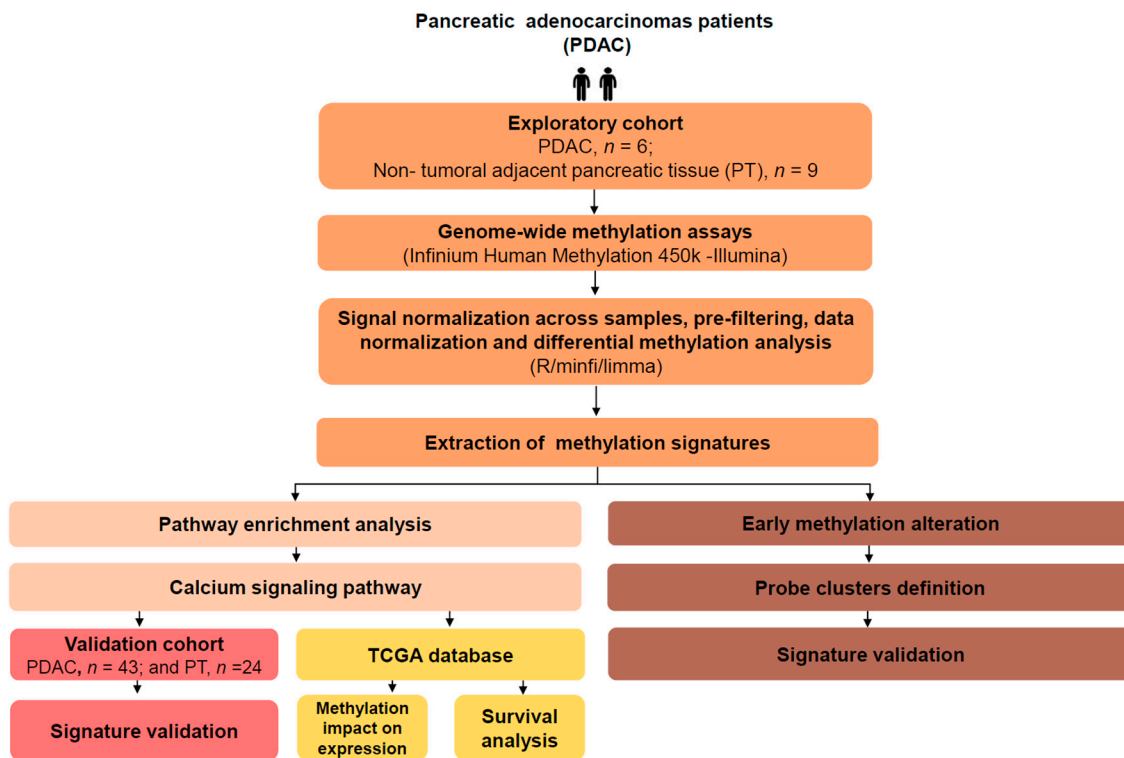
Finally, our data suggest that the dysregulation of  $\text{Ca}^{+2}$  signaling by epigenetic mechanisms is an early event in pancreatic carcinogenesis, reinforcing its relevance in this process. The stepwise methylation profile of *HRH1*, *CASQ2*, and *ORAI2*, together with twenty-one other genes that control the  $\text{Ca}^{2+}$  influx, were found in PT-like samples (Figures 4b–d and S4, Table S6). However, these alterations need to be validated in an independent longitudinal study, since they may not only shed light on the early molecular mechanisms driving PDAC development, but also represent potential biomarkers. DNA methylation alterations have been proposed as useful biomarkers due to their high sensitivity and specificity, and because they can be assessed by minimally invasive approaches, such as in liquid biopsies [86]. Therefore, our results bring the epigenetic dysregulation of the  $\text{Ca}^{+2}$  signaling pathway as a promising tool for PDAC management, either as diagnostic and prognostic biomarkers, or as therapeutic targets.

## 4. Materials and Methods

### 4.1. Patients and Sample Collection

Patients enrolled in this study were treated at Hospital de Clínicas de Porto Alegre (HCPA/UFRGS), in Southern Brazil between 2012 and 2018. Inclusion criteria were: pathology-proven diagnosis of PDAC, and no history of previous or current chemo- or radiation therapy. PDAC and PT samples were obtained during surgery or diagnostic biopsy procedures, and stored according to the biobank protocols from the hospital. Hematoxylin–eosin slides were prepared for all cases to confirm the diagnosis and assess the sample quality, which was performed by two pathologists (R.R. and S.M.). Samples with pancreatitis, necrosis, fibrosis and less than 20% cellularity were excluded [10]. The study was conducted in accordance with the Declaration of Helsinki, and the protocol was approved by the Ethics Committee of Hospital de Clínicas de Porto Alegre (Project Number: 2014–0526). All subjects gave their informed consent for inclusion before they participated in the study. Information about age at diagnosis, gender, TNM Classification of Malignant Tumors (TNM), classification, tumor location, and differentiation grade were obtained from the patient’s electronic medical record. Tumor location was categorized as pancreatic head vs. non-head.

We performed a genome-wide DNA methylation profiling in an exploratory cohort using the 450 K BeadChip Array platform (Illumina Infinium Human Methylation, San Diego, CA, USA). Six PDAC and nine PT samples with content (cellularity)  $\geq 70\%$  were included. Differentially methylated genes were selected, and validation was performed by pyrosequencing in a biological and technical validation cohort comprising a different set including 43 PDAC and 24 PT samples. The overall experimental design is summarized in Scheme 1.



**Scheme 1.** Flow chart illustrating the overall design of the study.

#### 4.2. DNA Isolation and Bisulfite Conversion

The PureLink Genomic DNA Kit (Thermo Fisher Scientific) was used to isolate the DNA from fresh frozen tissues according to the manufacturer's protocol and eluted DNA was quantified using Qubit V2.0 (Invitrogen, Carlsbad, USA). DNA from each sample was bisulfite converted using the EZ-DNA methylation kit (Zymo Research Corporation, California) according to the manufacturers' protocol.

#### 4.3. Human Methylation 450 K Array and Data Preprocessing

PDAC and PT tissues were used to establish an exploratory cohort. Illumina Infinium Human Methylation450 k (HM450 K) Bead-Chips (Illumina, San Diego, CA, USA) were used for investigating the genome-wide DNA methylation profile. Raw data were subjected to quality control, prefiltering, signal normalization across samples, and normalization using the funnorm function (R packages minfi) [87,88]. The Infinium data generated in this study were deposited in Gene Expression Omnibus (GEO) database and are available under accession number (GSE149250).

#### 4.4. Differential Methylation Analysis

Differential methylation analysis was performed with *limma* R/Bioconductor package, using the M-values matrix as input [89]. Correction for multiple testing was conducted with the Benjamini–Hochberg false discovery rate (FDR) procedure. Probes were annotated for approved gene symbols using annotation files provided by the manufacturer, and all probes with ambiguous annotations were removed from further analyses. The identification of DMPs in PDAC and PT samples was performed as previously described [90]. The DMPs were identified by using a cut-off of FDR-corrected  $p$ -values  $< 0.01$  and an absolute difference between the means of the  $\beta$ -values ( $\Delta\beta$ )  $\geq 0.2$ . To verify the methylation patterns in cases and controls, a hierarchical clustering analysis was applied to the M-values from DMPs using the complete linkage method and Euclidean distance, as implemented by the *heatmap.2* function from *gplots* R package.

#### 4.5. Functional Enrichment Analysis

DMPs were subject to functional enrichment analysis using pathway annotations from the KEGG [91,92] and the *clusterProfiler* package [93] in the R/Bioconductor environment. For this purpose, the gene symbol annotation of hyper- and hypomethylated probes were analyzed separately. Only the KEGG pathways with a minimum size of 30 annotated genes were considered for further analyses. Statistical significance for the enrichment of the KEGG pathways was estimated with a hypergeometric test and adjusted to account for the multiple hypotheses testing using the FDR procedure. Pathways with a FDR-corrected  $p$ -value  $< 0.05$  were highlighted as potentially enriched for hypo- or hypermethylated genes. Results were visualized using Cytoscape v3.4.0.

#### 4.6. Technical and Biologic Validation

In order to biologically and technically validate the array data, we performed the pyrosequencing (PyroMark Q96 ID-Qiagen) of selected  $\text{Ca}^{2+}$  pathway genes in tissue samples with  $\geq 20\%$  cellularity. Genes were chosen according to the following selection criteria: only genes with DMP which were exclusively hypo- or hypermethylated; genes associated with a high  $|\Delta\beta|$ ; and/or genes with previously described roles in carcinogenesis. After applying this filter, five genes were selected: *RYR3* (hypermethylated) and *CALM2*, *CAMK2A*, *ITPR2* and *EGFR* (all of them hypomethylated).

#### 4.7. TCGA Analysis

RNA-seq and methylation microarray (HM450 K) data were downloaded using the GDC Data Transfer Tool. Only patients who had both methylation and expression data for all the target genes were included. The unsupervised hierarchical clustering (heatmap with dendrograms) and KEGG pathway figures were built with the Complex Heatmap v.2.0 and KEGG graph v.1.44.0 packages, respectively, and the correlations (FDR-adjusted  $p$ -value  $< 0.05$ ) were performed with the psych v.1.8.12 package. The promoter category includes probes located in the genomic region TSS1500 and TSS200. All the PDAC samples with available mRNA data ( $n = 146$ ) were used to analyze the mRNA expression prognostic values of selected  $\text{Ca}^{2+}$  pathway genes in PDCA samples. Only stage IV cases ( $n = 4$ ) were excluded for being unresectable. The mRNA expression of selected genes was divided by tertiles and the lower and higher tertiles were used to classify cases into low and high expression, respectively. Genes for which more than one third of the cases had no detectable expression were analyzed by comparing the groups of patients with no detectable expression vs. patients with detectable expression. For the estimation of univariate survival, we used the Kaplan–Meier survival curve and statistical significance between the two groups was calculated by the log-rank test. Only genes with log-rank  $p$ -values  $< 0.05$  remained in the model. Lymph node invasion and residual tumor status after surgical resection were selected for multivariate analysis due to their statistically significant association with OS in the univariate analysis. Cox regression using the stepwise forward method was applied. All survival analyses were performed using the package “Survival” for R.

## 5. Conclusions

In summary, our results show that DNA methylation alterations are involved in the deregulation of the  $\text{Ca}^{2+}$  signaling pathway genes. These alterations impact gene expression, the overall survival of patients, and are already seen in tumor-adjacent tissue. Future studies should be performed to validate our findings, but the data presented here indicate a significant role of epigenetic alterations in the  $\text{Ca}^{2+}$  signaling pathway in PDAC.

**Supplementary Materials:** The following are available online at <http://www.mdpi.com/2072-6694/12/7/1735/s1>, Figure S1: Functional enrichment of differentially methylated genes in pancreatic adenocarcinoma, Figure S2: Validation of the genome-wide DNA methylation results with pyrosequencing, Figure S3: Non-tumoral pancreatic tissue -like (PT-like) analysis, Figure S4: Methylation levels of 24  $\text{Ca}^{2+}$  signaling pathway genes in PT, PT-like and PDAC samples, Table S1: Enriched KEGG terms for hypermethylated genes, Table S2: Enriched KEGG terms for hypomethylated genes, Table S3: PDAC clinicopathological features of the validation cohort ( $N = 43$ ), Table S4:

Correlation between probe methylation and gene expression, Table S5: Evaluation of the impact of the expression of Ca<sup>2+</sup> signaling genes on pancreatic ductal adenocarcinoma overall survival, Table S6: Analysis of early DNA methylation alterations, Table S7: Clinicopathological features of pancreatic ductal adenocarcinoma patients included in the exploratory and validation cohort.

**Author Contributions:** Conceptualization C.G., S.C.S.-L., and B.A.; methodology C.G., S.C.S.-L., B.A., R.R., S.M.; and A.O.; software S.C.S.-L., M.R.-M., D.C. and P.T.d.S.-S.; validation C.G., S.C.S.-L., and B.A.; formal analysis C.G., S.C.S.-L., and B.A.; data curation C.G., S.C.S.-L., and B.A.; writing—original draft preparation C.G., S.C.S.-L., B.A., M.R.-M., and P.A.-P.; writing—review and editing C.G., S.C.S.-L., B.A., M.R.-M., D.C., P.T.d.S.-S., R.R., S.M., A.O., P.A.-P., and L.F.R.P.; supervision P.A.-P.; and L.F.R.P.; All authors read and contributed, with a critical revision of the paper, to the final version of the manuscript. All authors have read and agreed to the published version of the manuscript.

**Funding:** The study was supported by Fundo de Incentivo à Pesquisa—FIPE, Hospital de Clínicas de Porto Alegre (GPPG Grant #14-0526), Instituto Nacional do Câncer, Conselho Nacional de Pesquisa (CNPq) universal (Grant #424646/2016-1), scholarships from CNPq, Coordenação de aperfeiçoamento de pessoal de nível superior (CAPES), Fundação de Amparo a Pesquisa do Estado do Rio de Janeiro (FAPERJ, Grant #E-26/010.001856/2015), and Swiss Bridge Foundation (Grant # 302404).

**Acknowledgments:** The authors thank Eduardo Chiela, Yasminne Rocha, Ivaine Sauthier, Tiago Finger Andreis, Igor Araujo Vieira, Marina Nicolau and Paula Vieira for technical support and stimulating discussions, and CNPq/Rede Genoprot (#559814/2009-7).

**Conflicts of Interest:** All authors declare no potential financial or ethical conflicts of interest regarding the contents of this submission.

## Abbreviations

<i>ADCY8</i>	Adenylate Cyclase 8
<i>ADRA1A</i>	Adrenoceptor Alpha 1A
<i>AGTR1</i>	Angiotensin II Receptor Type 1
ASICs	Acid-Sensing Ion Channels
Ca <sup>2+</sup>	Calcium
<i>CACNA1A</i>	Calcium Voltage-Gated Channel Subunit Alpha1 A
<i>CACNA1B</i>	Calcium Voltage-Gated Channel Subunit Alpha1 B
<i>CACNA1C</i>	Calcium Voltage-Gated Channel Subunit Alpha1 C
<i>CACNA1D</i>	Calcium Voltage-Gated Channel Subunit Alpha1 D
<i>CACNA1H</i>	Calcium Voltage-Gated Channel Subunit Alpha1 H
<i>CALM2</i>	Calmodulin 2
<i>CAMK2A</i>	Calcium/Calmodulin Dependent Protein Kinase II Alpha
<i>CAMKK1</i>	Calcium/Calmodulin Dependent Protein Kinase Kinase 1
<i>CASQ2</i>	Calsequestrin 2
<i>CDO1</i>	Cysteine Dioxygenase Type 1
CRAC	Calcium Release-Activated Calcium Channels
DMPs	Differentially Methylated Probes
<i>EGFR</i>	Epidermal Growth Factor Receptor
ER	Endoplasmic Reticulum
FAK	Focal Adhesion Kinase
FDR	False Discovery Rate
<i>FOXE1</i>	Forkhead Box E1
GEO	Gene Expression Omnibus
<i>GRIN2A</i>	Glutamate Ionotropic Receptor NMDA Type Subunit 2A
HM450K	Human Methylation 450k
HR	Hazard Ratio
<i>HRH1</i>	Histamine Receptor H1
IP <sub>3</sub>	Inositol-1,4,5-Trisphosphate
IP <sub>3</sub> Rs	Inositol 1,4,5-Trisphosphate Receptors
<i>ITPKB</i>	Inositol-Trisphosphate 3-Kinase B
<i>ITPR1</i>	Inositol 1,4,5-Trisphosphate Receptor Type 1
<i>ITPR2</i>	Inositol 1,4,5-Trisphosphate Receptor Type 2
KEGG	Kyoto Encyclopedia of Genes and Genomes



KRAS	KRAS Proto-Oncogene, GTPase
Mg <sup>2+</sup>	Magnesium
NHE1	Sodium/Proton Exchanger-1
NPTX2	Neuronal Pentraxin 2
ORAI1	ORAI Calcium Release-Activated Calcium Modulator 1
ORAI2	ORAI Calcium Release-Activated Calcium Modulator 2
OS	Overall Survival
P2RX2	Purinergic Receptor P2X 2
PCDH10	Protocadherin 10
PDAC	Pancreatic Ductal Adenocarcinoma
PDE1C	Phosphodiesterase 1C
PENK	Proenkephalin
PLCB1	Phospholipase C Beta 1
PRKCB	Protein Kinase C Beta
PT	Pancreatic Non-Tumoral Tissue
PT-LIKE	Pancreatic Non-Tumoral-Like Tissue
RSEM	RNA-Seq by Expectation-Maximization
RYR2	Ryanodine Receptor 2
RYR3	Ryanodine Receptor 3
RyRs	Ryanodine Receptors
S100A4	S100 Calcium Binding Protein A4
SERCA	Sarcoendoplasmic Reticulum Ca <sup>2+</sup> ATPases
SFRP1	Secreted Frizzled Related Protein 1
SFRP2	Secreted Frizzled Related Protein 2
SLC8A3	Solute Carrier Family 8 Member A3
SOCE	Store Operated Calcium Entry
STIM	Stromal Interaction Molecule
STIM	Stromal Interaction Molecule 1
TCGA	Cancer Genome Atlas
TFPI2	Tissue Factor Pathway Inhibitor 2
TNM	TNM Classification of Malignant Tumors
TRPCs	Transient Receptor Potential Channels
TRPVs	Transient Receptor Potential Vanilloid Channels
TSGs	Tumor Suppressor Genes
UTR	Untranslated Region

## References

- Collisson, E.A.; Maitra, A. Pancreatic Cancer Genomics 2.0: Profiling Metastases. *Cancer Cell* **2017**, *31*, 309–310. [[CrossRef](#)]
- Siegel, R.L.; Miller, K.D.; Jemal, A. Cancer statistics, 2018. *CA Cancer J. Clin.* **2018**, *68*, 7–30. [[CrossRef](#)] [[PubMed](#)]
- Chakraborty, S.; Baine, M.J.; Sasson, A.R.; Batra, S.K. Current status of molecular markers for early detection of sporadic pancreatic cancer. *Biochim. Biophys. Acta* **2011**, *1815*, 44–64. [[CrossRef](#)]
- Rahib, L.; Smith, B.D.; Aizenberg, R.; Rosenzweig, A.B.; Fleshman, J.M.; Matrisian, L.M. Projecting cancer incidence and deaths to 2030: The unexpected burden of thyroid, liver, and pancreas cancers in the United States. *Cancer Res.* **2014**, *74*, 2913–2921. [[CrossRef](#)] [[PubMed](#)]
- Kleeff, J.; Korc, M.; Apte, M.; La Vecchia, C.; Johnson, C.D.; Biankin, A.V.; Neale, R.E.; Tempero, M.; Tuveson, D.A.; Hruban, R.H.; et al. Pancreatic cancer. *Nat. Rev. Dis. Prim.* **2016**, *2*, 16022. [[CrossRef](#)] [[PubMed](#)]
- Orth, M.; Metzger, P.; Gerum, S.; Mayerle, J.; Schneider, G.; Belka, C.; Schnurr, M.; Lauber, K. Pancreatic ductal adenocarcinoma: Biological hallmarks, current status, and future perspectives of combined modality treatment approaches. *Radiat. Oncol.* **2019**, *14*, 141. [[CrossRef](#)]
- Ehrlich, M. DNA hypomethylation in cancer cells. *Epigenomics* **2009**, *1*, 239–259. [[CrossRef](#)]

8. Wang, X.-X.; Xiao, F.-H.; Li, Q.-G.; Liu, J.; He, Y.-H.; Kong, Q.-P. Large-scale DNA methylation expression analysis across 12 solid cancers reveals hypermethylation in the calcium-signaling pathway. *Oncotarget* **2017**, *8*, 11868–11876. [[CrossRef](#)]
9. Ahuja, N.; Sharma, A.R.; Baylin, S.B. Epigenetic Therapeutics: A New Weapon in the War Against Cancer. *Annu. Rev. Med.* **2016**, *67*, 73–89. [[CrossRef](#)]
10. Nones, K.; Waddell, N.; Song, S.; Patch, A.-M.; Miller, D.; Johns, A.; Wu, J.; Kassahn, K.S.; Wood, D.; Bailey, P.; et al. Genome-wide DNA methylation patterns in pancreatic ductal adenocarcinoma reveal epigenetic deregulation of SLIT-ROBO, ITGA2 and MET signaling. *Int. J. cancer* **2014**, *135*, 1110–1118. [[CrossRef](#)]
11. Mishra, N.K.; Guda, C. Genome-wide DNA methylation analysis reveals molecular subtypes of pancreatic cancer. *Oncotarget* **2017**, *8*, 28990–29012. [[CrossRef](#)] [[PubMed](#)]
12. Boutros, T.; Chevet, E.; Metrakos, P. Mitogen-activated protein (MAP) kinase/MAP kinase phosphatase regulation: Roles in cell growth, death, and cancer. *Pharmacol. Rev.* **2008**, *60*, 261–310. [[CrossRef](#)] [[PubMed](#)]
13. Maziveyi, M.; Alahari, S.K. Cell matrix adhesions in cancer: The proteins that form the glue. *Oncotarget* **2017**, *8*, 48471–48487. [[CrossRef](#)] [[PubMed](#)]
14. Xu, M.; Seas, A.; Kiyani, M.; Ji, K.S.Y.; Bell, H.N. A temporal examination of calcium signaling in cancer—from tumorigenesis, to immune evasion, and metastasis. *Cell Biosci.* **2018**, *8*, 25. [[CrossRef](#)]
15. Network, C.G.A.R. Integrated Genomic Characterization of Pancreatic Ductal Adenocarcinoma. *Cancer Cell* **2017**, *32*, 185.e13–203.e13.
16. Curtius, K.; Wright, N.A.; Graham, T.A. An evolutionary perspective on field cancerization. *Nat. Rev. Cancer* **2018**, *18*, 19–32. [[CrossRef](#)]
17. Baylin, S.B.; Jones, P.A. A decade of exploring the cancer epigenome—biological and translational implications. *Nat. Rev. Cancer* **2011**, *11*, 726–734. [[CrossRef](#)]
18. Yamashita, K.; Hosoda, K.; Nishizawa, N.; Katoh, H.; Watanabe, M. Epigenetic biomarkers of promoter DNA methylation in the new era of cancer treatment. *Cancer Sci.* **2018**, *109*, 3695–3706. [[CrossRef](#)]
19. Nishizawa, N.; Harada, H.; Kumamoto, Y.; Kaizu, T.; Katoh, H.; Tajima, H.; Ushiku, H.; Yokoi, K.; Igarashi, K.; Fujiyama, Y.; et al. Diagnostic potential of hypermethylation of the cysteine dioxygenase 1 gene (CDO1) promoter DNA in pancreatic cancer. *Cancer Sci.* **2019**. [[CrossRef](#)]
20. Kinugawa, Y.; Uehara, T.; Sano, K.; Matsuda, K.; Maruyama, Y.; Kobayashi, Y.; Nakajima, T.; Hamano, H.; Kawa, S.; Higuchi, K.; et al. Methylation of Tumor Suppressor Genes in Autoimmune Pancreatitis. *Pancreas* **2017**, *46*, 614–618. [[CrossRef](#)]
21. Matsubayashi, H.; Canto, M.; Sato, N.; Klein, A.; Abe, T.; Yamashita, K.; Yeo, C.J.; Kallou, A.; Hruban, R.; Goggins, M. DNA methylation alterations in the pancreatic juice of patients with suspected pancreatic disease. *Cancer Res.* **2006**, *66*, 1208–1217. [[CrossRef](#)] [[PubMed](#)]
22. Yang, L.; Yang, H.; Li, J.; Hao, J.; Qian, J. ppENK Gene Methylation Status in the Development of Pancreatic Carcinoma. *Gastroenterol. Res. Pr.* **2013**, *2013*, 130927.
23. Brune, K.; Hong, S.M.; Li, A.; Yachida, S.; Abe, T.; Griffith, M.; Yang, D.; Omura, N.; Eshleman, J.; Canto, M.; et al. Genetic and epigenetic alterations of familial pancreatic cancers. *Cancer Epidemiol. Biomarkers Prev.* **2008**, *17*, 3536–3542. [[CrossRef](#)] [[PubMed](#)]
24. Sato, N.; Fukushima, N.; Maitra, A.; Matsubayashi, H.; Yeo, C.J.; Cameron, J.L.; Hruban, R.H.; Goggins, M. Discovery of novel targets for aberrant methylation in pancreatic carcinoma using high-throughput microarrays. *Cancer Res.* **2003**, *63*, 3735–3742.
25. Berridge, M.J.; Lipp, P.; Bootman, M.D. The versatility and universality of calcium signalling. *Nat. Rev. Mol. Cell Biol.* **2000**, *1*, 11–21. [[CrossRef](#)]
26. Li, H.; Liu, J.-W.; Liu, S.; Yuan, Y.; Sun, L.-P. Bioinformatics-Based Identification of Methylated-Differentially Expressed Genes and Related Pathways in Gastric Cancer. *Dig. Dis. Sci.* **2017**, *62*, 3029–3039. [[CrossRef](#)]
27. Pedriali, G.; Rimessi, A.; Sbano, L.; Giorgi, C.; Wieckowski, M.R.; Pleviati, M.; Pinton, P. Regulation of Endoplasmic Reticulum-Mitochondria Ca. *Front. Oncol.* **2017**, *7*, 180. [[CrossRef](#)]
28. Bootman, M.D. Calcium signaling. *Cold Spring Harb. Perspect Biol.* **2012**, *4*, a011171. [[CrossRef](#)]
29. Eichberg, J.; Zhu, M.X. *Calcium Entry Channels in Non-Excitable Cells*, 1st ed.; Kozak, J.A., Putney, J.W.J., Eds.; CRC Press: Boca Raton, FL, USA, 2018; ISBN 9781315152592.

30. Feber, A.; Clark, J.; Goodwin, G.; Dodson, A.R.; Smith, P.H.; Fletcher, A.; Edwards, S.; Flohr, P.; Falconer, A.; Roe, T.; et al. Amplification and overexpression of E2F3 in human bladder cancer. *Oncogene* **2004**, *23*, 1627–1630. [[CrossRef](#)]
31. Holcomb, I.N.; Young, J.M.; Coleman, I.M.; Salari, K.; Grove, D.I.; Hsu, L.; True, L.D.; Roudier, M.P.; Morrissey, C.M.; Higano, C.S.; et al. Comparative analyses of chromosome alterations in soft-tissue metastases within and across patients with castration-resistant prostate cancer. *Cancer Res.* **2009**, *69*, 7793–7802. [[CrossRef](#)]
32. Monteith, G.R.; Davis, F.M.; Roberts-Thomson, S.J. Calcium channels and pumps in cancer: Changes and consequences. *J. Biol. Chem.* **2012**, *287*, 31666–31673. [[CrossRef](#)] [[PubMed](#)]
33. Monteith, G.R.; McAndrew, D.; Faddy, H.M.; Roberts-Thomson, S.J. Calcium and cancer: Targeting Ca<sup>2+</sup> transport. *Nat. Rev. Cancer* **2007**, *7*, 519–530. [[CrossRef](#)]
34. Ibrahim, S.; Dakik, H.; Vandier, C.; Chautard, R.; Paintaud, G.; Mazurier, F.; Lecomte, T.; Guéguinou, M.; Raoul, W. Expression Profiling of Calcium Channels and Calcium-Activated Potassium Channels in Colorectal Cancer. *Cancers (Basel)* **2019**, *11*, 561. [[CrossRef](#)]
35. McAndrew, D.; Grice, D.M.; Peters, A.A.; Davis, F.M.; Stewart, T.; Rice, M.; Smart, C.E.; Brown, M.A.; Kenny, P.A.; Roberts-Thomson, S.J.; et al. ORAI1-mediated calcium influx in lactation and in breast cancer. *Mol. Cancer Ther.* **2011**, *10*, 448–460. [[CrossRef](#)] [[PubMed](#)]
36. Crottès, D.; Lin, Y.T.; Peters, C.J.; Gilchrist, J.M.; Wiita, A.P.; Jan, Y.N.; Jan, L.Y. TMEM16A controls EGF-induced calcium signaling implicated in pancreatic cancer prognosis. *Proc. Natl. Acad. Sci. USA* **2019**, *116*, 13026–13035. [[CrossRef](#)] [[PubMed](#)]
37. Chen, Y.F.; Chen, Y.T.; Chiu, W.T.; Shen, M.R. Remodeling of calcium signaling in tumor progression. *J. Biomed. Sci.* **2013**, *20*, 23. [[CrossRef](#)] [[PubMed](#)]
38. Raynal, N.J.; Lee, J.T.; Wang, Y.; Beaudry, A.; Madireddi, P.; Garriga, J.; Malouf, G.G.; Dumont, S.; Dettman, E.J.; Gharibyan, V.; et al. Targeting Calcium Signaling Induces Epigenetic Reactivation of Tumor Suppressor Genes in Cancer. *Cancer Res.* **2016**, *76*, 1494–1505. [[CrossRef](#)] [[PubMed](#)]
39. Deliot, N.; Constantin, B. Plasma membrane calcium channels in cancer: Alterations and consequences for cell proliferation and migration. *Biochim. Biophys. Acta* **2015**, *1848*, 2512–2522. [[CrossRef](#)]
40. Roberts-Thomson, S.J.; Chalmers, S.B.; Monteith, G.R. The Calcium-Signaling Toolkit in Cancer: Remodeling and Targeting. *Cold Spring Harb. Perspect. Biol.* **2019**, *11*. [[CrossRef](#)]
41. Boye, K.; Maelandsmo, G.M. S100A4 and metastasis: A small actor playing many roles. *Am. J. Pathol.* **2010**, *176*, 528–535. [[CrossRef](#)]
42. Rosty, C.; Ueki, T.; Argani, P.; Jansen, M.; Yeo, C.J.; Cameron, J.L.; Hruban, R.H.; Goggins, M. Overexpression of S100A4 in pancreatic ductal adenocarcinomas is associated with poor differentiation and DNA hypomethylation. *Am. J. Pathol.* **2002**, *160*, 45–50. [[CrossRef](#)]
43. Qiu, C.; Bu, X.; Jiang, Z. Protocadherin-10 acts as a tumor suppressor gene, and is frequently downregulated by promoter methylation in pancreatic cancer cells. *Oncol. Rep.* **2016**, *36*, 383–389. [[CrossRef](#)]
44. Curia, M.C.; Fantini, F.; Lattanzio, R.; Tavano, F.; Di Mola, F.; Piantelli, M.; Battista, P.; Di Sebastiano, P.; Cama, A. High methylation levels of PCDH10 predict poor prognosis in patients with pancreatic ductal adenocarcinoma. *BMC Cancer* **2019**, *19*, 452. [[CrossRef](#)]
45. Nguyen, N.T.; Han, W.; Cao, W.-M.; Wang, Y.; Wen, S.; Huang, Y.; Li, M.; Du, L.; Zhou, Y. Store-Operated Calcium Entry Mediated by ORAI and STIM. *Compr. Physiol.* **2018**, *8*, 981–1002. [[PubMed](#)]
46. Kondratska, K.; Kondratskyi, A.; Yassine, M.; Lemonnier, L.; Lepage, G.; Morabito, A.; Skryma, R.; Prevarskaya, N. Orai1 and STIM1 mediate SOCE and contribute to apoptotic resistance of pancreatic adenocarcinoma. *Biochim. Biophys. Acta* **2014**, *1843*, 2263–2269. [[CrossRef](#)] [[PubMed](#)]
47. Khan, H.Y.; Mpilla, G.B.; Sexton, R.; Viswanadha, S.; Penmetsa, K.V.; Aboukameel, A.; Diab, M.; Kamgar, M.; Al-Hallak, M.N.; Szlachky, M.; et al. Calcium Release-Activated Calcium (CRAC) Channel Inhibition Suppresses Pancreatic Ductal Adenocarcinoma Cell Proliferation and Patient-Derived Tumor Growth. *Cancers (Basel)* **2020**, *12*, 750. [[CrossRef](#)] [[PubMed](#)]
48. Roderick, H.L.; Cook, S.J. Ca<sup>2+</sup> signalling checkpoints in cancer: Remodelling Ca<sup>2+</sup> for cancer cell proliferation and survival. *Nat. Rev. Cancer* **2008**, *8*, 361–375. [[CrossRef](#)]
49. Yarden, Y. The EGFR family and its ligands in human cancer. signalling mechanisms and therapeutic opportunities. *Eur. J. Cancer* **2001**, *37* (Suppl. S4), S3–S8. [[CrossRef](#)]

50. Cui, C.; Merritt, R.; Fu, L.; Pan, Z. Targeting calcium signaling in cancer therapy. *Acta Pharm. Sin. B* **2017**, *7*, 3–17. [[CrossRef](#)]
51. Navas, C.; Hernández-Porras, I.; Schuhmacher, A.J.; Sibilía, M.; Guerra, C.; Barbacid, M. EGF receptor signaling is essential for k-ras oncogene-driven pancreatic ductal adenocarcinoma. *Cancer Cell* **2012**, *22*, 318–330. [[CrossRef](#)]
52. Balsano, R.; Tommasi, C.; Garajova, I. State of the Art for Metastatic Pancreatic Cancer Treatment: Where Are We Now? *Anticancer Res.* **2019**, *39*, 3405–3412. [[CrossRef](#)] [[PubMed](#)]
53. Shi, J.L.; Fu, L.; Wang, W.D. High expression of inositol 1,4,5-trisphosphate receptor, type 2 (ITPR2) as a novel biomarker for worse prognosis in cytogenetically normal acute myeloid leukemia. *Oncotarget* **2015**, *6*, 5299–5309. [[CrossRef](#)] [[PubMed](#)]
54. Prior, I.A.; Lewis, P.D.; Mattos, C. A comprehensive survey of Ras mutations in cancer. *Cancer Res.* **2012**, *72*, 2457–2467. [[CrossRef](#)] [[PubMed](#)]
55. Schaal, C.; Padmanabhan, J.; Chellappan, S. The Role of nAChR and Calcium Signaling in Pancreatic Cancer Initiation and Progression. *Cancers (Basel)* **2015**, *7*, 1447–1471. [[CrossRef](#)]
56. Lanner, J.T.; Georgiou, D.K.; Joshi, A.D.; Hamilton, S.L. Ryanodine receptors: Structure, expression, molecular details, and function in calcium release. *Cold Spring Harb. Perspect Biol.* **2010**, *2*, a003996. [[CrossRef](#)]
57. Brzozowski, J.S.; Skelding, K.A. The Multi-Functional Calcium/Calmodulin Stimulated Protein Kinase (CaMK) Family: Emerging Targets for Anti-Cancer Therapeutic Intervention. *Pharmaceuticals* **2019**, *12*, 8. [[CrossRef](#)]
58. Wang, Y.Y.; Zhao, R.; Zhe, H. The emerging role of CaMKII in cancer. *Oncotarget* **2015**, *6*, 11725–11734. [[CrossRef](#)]
59. Tai, Y.L.; Chen, L.C.; Shen, T.L. Emerging roles of focal adhesion kinase in cancer. *Biomed. Res. Int.* **2015**, *2015*, 690690. [[CrossRef](#)]
60. Chen, W.; An, P.; Quan, X.-J.; Zhang, J.; Zhou, Z.-Y.; Zou, L.-P.; Luo, H.-S. Ca(2+)/calmodulin-dependent protein kinase II regulates colon cancer proliferation and migration via ERK1/2 and p38 pathways. *World J. Gastroenterol.* **2017**, *23*, 6111–6118. [[CrossRef](#)]
61. Bouchard, V.; Demers, M.J.; Thibodeau, S.; Laquerre, V.; Fujita, N.; Tsuruo, T.; Beaulieu, J.F.; Gauthier, R.; Vézina, A.; Villeneuve, L.; et al. Fak/Src signaling in human intestinal epithelial cell survival and anoikis: Differentiation state-specific uncoupling with the PI3-K/Akt-1 and MEK/Erk pathways. *J. Cell Physiol.* **2007**, *212*, 717–728. [[CrossRef](#)]
62. Ma, X.; Cai, Y.; He, D.; Zou, C.; Zhang, P.; Lo, C.Y.; Xu, Z.; Chan, F.L.; Yu, S.; Chen, Y.; et al. Transient receptor potential channel TRPC5 is essential for P-glycoprotein induction in drug-resistant cancer cells. *Proc. Natl. Acad. Sci. USA* **2012**, *109*, 16282–16287. [[CrossRef](#)] [[PubMed](#)]
63. Zhang, S.; Miao, Y.; Zheng, X.; Gong, Y.; Zhang, J.; Zou, F.; Cai, C. STIM1 and STIM2 differently regulate endogenous Ca(2+) entry and promote TGF- $\beta$ -induced EMT in breast cancer cells. *Biochem. Biophys. Res. Commun.* **2017**, *488*, 74–80. [[CrossRef](#)] [[PubMed](#)]
64. Zhu, S.; Zhou, H.-Y.; Deng, S.-C.; Deng, S.-J.; He, C.; Li, X.; Chen, J.-Y.; Jin, Y.; Hu, Z.-L.; Wang, F.; et al. ASIC1 and ASIC3 contribute to acidity-induced EMT of pancreatic cancer through activating Ca(2+)/RhoA pathway. *Cell Death Dis.* **2017**, *8*, e2806. [[CrossRef](#)] [[PubMed](#)]
65. Bhattacharya, A.; Kumar, J.; Hermanson, K.; Sun, Y.; Qureshi, H.; Perley, D.; Scheidegger, A.; Singh, B.B.; Dhasarathy, A. The calcium channel proteins ORAI3 and STIM1 mediate TGF- $\beta$  induced Snai1 expression. *Oncotarget* **2018**, *9*, 29468–29483. [[CrossRef](#)]
66. Porcelli, L.; Iacobazzi, R.M.; Di Fonte, R.; Serratì, S.; Intini, A.; Solimando, A.G.; Brunetti, O.; Calabrese, A.; Leonetti, F.; Azzariti, A.; et al. CAFs and TGF- $\beta$  Signaling Activation by Mast Cells Contribute to Resistance to Gemcitabine/Nabpaclitaxel in Pancreatic Cancer. *Cancers (Basel)* **2019**, *11*, 330. [[CrossRef](#)]
67. Köster, S.; Pavkov-Keller, T.; Kühlbrandt, W.; Yildiz, Ö. Structure of human Na<sup>+</sup>/H<sup>+</sup> exchanger NHE1 regulatory region in complex with calmodulin and Ca<sup>2+</sup>. *J. Biol. Chem.* **2011**, *286*, 40954–40961. [[CrossRef](#)] [[PubMed](#)]
68. Argentiero, A.; De Summa, S.; Di Fonte, R.; Iacobazzi, M.R.; Porcelli, L.; Da Vià, M.; Brunetti, O.; Azzariti, A.; Silvestris, N.; Solimando, G.A. Gene Expression Comparison between the Lymph Node-Positive and -Negative Reveals a Peculiar Immune Microenvironment Signature and a Theranostic Role for WNT Targeting in Pancreatic Ductal Adenocarcinoma: A Pilot Study. *Cancers* **2019**, *11*, 942. [[CrossRef](#)] [[PubMed](#)]

69. Martinez-Bosch, N.; Vinaixa, J.; Navarro, P. Immune Evasion in Pancreatic Cancer: From Mechanisms to Therapy. *Cancers* **2018**, *10*, 6. [[CrossRef](#)]
70. Anderson, K.G.; Stromnes, I.M.; Greenberg, P.D. Obstacles Posed by the Tumor Microenvironment to T cell Activity: A Case for Synergistic Therapies. *Cancer Cell* **2017**, *31*, 311–325. [[CrossRef](#)]
71. Zhang, Q.; Lou, Y.; Zhang, J.; Fu, Q.; Wei, T.; Sun, X.; Chen, Q.; Yang, J.; Bai, X.; Liang, T. Hypoxia-inducible factor-2 $\alpha$  promotes tumor progression and has crosstalk with Wnt/ $\beta$ -catenin signaling in pancreatic cancer. *Mol. Cancer* **2017**, *16*, 119. [[CrossRef](#)]
72. Camuzi, D.; de Amorim, Í.S.S.; Ribeiro Pinto, L.F.; Oliveira Trivilin, L.; Mencialha, A.L.; Soares Lima, S.C. Regulation Is in the Air: The Relationship between Hypoxia and Epigenetics in Cancer. *Cells* **2019**, *8*, 300. [[CrossRef](#)] [[PubMed](#)]
73. Maftouh, M.; Belo, A.I.; Avan, A.; Funel, N.; Peters, G.J.; Giovannetti, E.; Van Die, I. Galectin-4 expression is associated with reduced lymph node metastasis and modulation of Wnt/ $\beta$ -catenin signalling in pancreatic adenocarcinoma. *Oncotarget* **2014**, *5*, 5335–5349. [[CrossRef](#)] [[PubMed](#)]
74. De, A. Wnt/ $\text{Ca}^{2+}$  signaling pathway: A brief overview. *Acta Biochim. Biophys. Sin. (Shanghai)* **2011**, *43*, 745–756. [[CrossRef](#)]
75. Bong, A.H.L.; Monteith, G.R. Calcium signaling and the therapeutic targeting of cancer cells. *Biochim. Biophys. Acta. Mol. Cell Res.* **2018**, *1865*, 1786–1794. [[CrossRef](#)] [[PubMed](#)]
76. Yang, S.; Zhang, J.J.; Huang, X.-Y. Orai1 and STIM1 are critical for breast tumor cell migration and metastasis. *Cancer Cell* **2009**, *15*, 124–134. [[CrossRef](#)]
77. Sallán, M.C.; Visa, A.; Shaikh, S.; Nàger, M.; Herreros, J.; Cantí, C. T-type  $\text{Ca}^{2+}$  Channels: T for Targetable. *Cancer Res.* **2018**, *78*, 603–609. [[CrossRef](#)]
78. Peters, A.A.; Jamaludin, S.Y.N.; Yapa, K.T.D.S.; Chalmers, S.; Wiegman, A.P.; Lim, H.F.; Milevskiy, M.J.G.; Azimi, I.; Davis, F.M.; Northwood, K.S.; et al. Oncosis and apoptosis induction by activation of an overexpressed ion channel in breast cancer cells. *Oncogene* **2017**, *36*, 6490–6500. [[CrossRef](#)]
79. Zhang, L.; Barritt, G.J. Evidence that TRPM8 is an androgen-dependent  $\text{Ca}^{2+}$  channel required for the survival of prostate cancer cells. *Cancer Res.* **2004**, *64*, 8365–8373. [[CrossRef](#)]
80. Tang, B.-D.; Xia, X.; Lv, X.-F.; Yu, B.-X.; Yuan, J.-N.; Mai, X.-Y.; Shang, J.-Y.; Zhou, J.-G.; Liang, S.-J.; Pang, R.-P. Inhibition of Orai1-mediated  $\text{Ca}^{2+}$  entry enhances chemosensitivity of HepG2 hepatocarcinoma cells to 5-fluorouracil. *J. Cell. Mol. Med.* **2017**, *21*, 904–915. [[CrossRef](#)] [[PubMed](#)]
81. Dziegielewska, B.; Casarez, E.V.; Yang, W.Z.; Gray, L.S.; Dziegielewski, J.; Slack-Davis, J.K. T-Type  $\text{Ca}^{2+}$  Channel Inhibition Sensitizes Ovarian Cancer to Carboplatin. *Mol. Cancer Ther.* **2016**, *15*, 460–470. [[CrossRef](#)]
82. Whitaker, M. Calcium at fertilization and in early development. *Physiol. Rev.* **2006**, *86*, 25–88. [[CrossRef](#)] [[PubMed](#)]
83. Chiappinelli, K.B.; Strissel, P.L.; Desrichard, A.; Li, H.; Henke, C.; Akman, B.; Hein, A.; Rote, N.S.; Cope, L.M.; Snyder, A.; et al. Inhibiting DNA Methylation Causes an Interferon Response in Cancer via dsRNA Including Endogenous Retroviruses. *Cell* **2016**, *164*, 1073. [[CrossRef](#)] [[PubMed](#)]
84. Roulois, D.; Loo Yau, H.; Singhanian, R.; Wang, Y.; Danesh, A.; Shen, S.Y.; Han, H.; Liang, G.; Jones, P.A.; Pugh, T.J.; et al. DNA-Demethylating Agents Target Colorectal Cancer Cells by Inducing Viral Mimicry by Endogenous Transcripts. *Cell* **2015**, *162*, 961–973. [[CrossRef](#)] [[PubMed](#)]
85. Jones, P.A.; Ohtani, H.; Chakravarthy, A.; De Carvalho, D.D. Epigenetic therapy in immune-oncology. *Nat. Rev. Cancer* **2019**, *19*, 151–161. [[CrossRef](#)] [[PubMed](#)]
86. Gai, W.; Sun, K. Epigenetic Biomarkers in Cell-Free DNA and Applications in Liquid Biopsy. *Genes (Basel)* **2019**, *10*, 32. [[CrossRef](#)]
87. Aryee, M.J.; Jaffe, A.E.; Corrada-Bravo, H.; Ladd-Acosta, C.; Feinberg, A.P.; Hansen, K.D.; Irizarry, R.A. Minfi: A flexible and comprehensive Bioconductor package for the analysis of Infinium DNA methylation microarrays. *Bioinformatics* **2014**, *30*, 1363–1369. [[CrossRef](#)]
88. Fortin, J.P.; Labbe, A.; Lemire, M.; Zanke, B.W.; Hudson, T.J.; Fertig, E.J.; Greenwood, C.M.; Hansen, K.D. Functional normalization of 450k methylation array data improves replication in large cancer studies. *Genome Biol.* **2014**, *15*, 503. [[CrossRef](#)]
89. Du, P.; Zhang, X.; Huang, C.-C.; Jafari, N.; Kibbe, W.A.; Hou, L.; Lin, S.M. Comparison of Beta-value and M-value methods for quantifying methylation levels by microarray analysis. *BMC Bioinform.* **2010**, *11*, 587. [[CrossRef](#)]

90. Martin, M.; Ancey, P.B.; Cros, M.P.; Durand, G.; Le Calvez-Kelm, F.; Hernandez-Vargas, H.; Herceg, Z. Dynamic imbalance between cancer cell subpopulations induced by transforming growth factor beta (TGF- $\beta$ ) is associated with a DNA methylome switch. *BMC Genom.* **2014**, *15*, 435. [[CrossRef](#)]
91. Kanehisa, M.; Goto, S. KEGG: Kyoto encyclopedia of genes and genomes. *Nucleic Acids Res.* **2000**, *28*, 27–30. [[CrossRef](#)]
92. Kanehisa, M.; Sato, Y.; Kawashima, M.; Furumichi, M.; Tanabe, M. KEGG as a reference resource for gene and protein annotation. *Nucleic Acids Res.* **2016**, *44*, D457–D462. [[CrossRef](#)] [[PubMed](#)]
93. Yu, G.; Wang, L.G.; Han, Y.; He, Q.Y. clusterProfiler: An R package for comparing biological themes among gene clusters. *OMICS* **2012**, *16*, 284–287. [[CrossRef](#)] [[PubMed](#)]



© 2020 by the authors. Licensee MDPI, Basel, Switzerland. This article is an open access article distributed under the terms and conditions of the Creative Commons Attribution (CC BY) license (<http://creativecommons.org/licenses/by/4.0/>).